Measurement of the thermal conductivity of flexible biosourced polymers using the 3-omega method

G. Boussatour[a], P.Y. Cresson[a,b,*], B. Genestie[b,c], N. Joly[b], J.F. Brun[d], T. Lasri[a]

[a] Univ. Lille, CNRS, Centrale Lille, ISEN, Univ. Valenciennes, UMR 8520 - IEMN, F-59000, Lille, France
[b] Univ. Artois, IUT Béthune, F-62408, Béthune, France
[c] Univ. Artois, EA 4515, Laboratoire de Génie Civil et géo-Environment (LGCgE), F-62400, Béthune, France
[d] Univ. Lille, CNRS, INRA, ENSCL, UMR 8207 - UMET - Unité Matériaux et Transformations, F-59000, Lille, France

ABSTRACT

The thermal conductivity of flexible biosourced polymers was measured by the 3-omega method. Two biopolymers were investigated: the polylactic acid (PLA), a widely used commercial biodegradable one, and the cellulose palmitate (CP), a hydrophobic biosourced material developed in the laboratory, that could be used in electronic or microfluidic applications. The 3-omega method is based-on the use of a metal element as both heating device to thermally disturb the system and temperature sensor. A stencil lithography technique was applied to obtain metallic lines, since biopolymers are not compatible with classical photolithography method. Thermal conductivities of 0.19 and 0.30 W/m.K are obtained respectively for PLA and CP thick films, and 0.12 and 0.22 W/m.K for respectively PLA and CP thin films. These values are close to those measured for petro-sourced substrates or films and so give the possibility to address the applications mentioned.

1. Introduction

Bio-based polymers have attracted significant attention in recent years, because of their properties, such as high biocompatibility, good mechanical and dielectric properties, flexibility, low weight and optical clarity compatible with commodity plastic market [1]. Bio-based polymers are obtained from renewable resources by (*i*) biological synthesis (ex: polyhydroxybutyrate PHB), (*ii*) chemical synthetic pathway (ex: PLA, Braskem polyethylene) or (*iii*) extraction from plant resources (polysaccharides, lignins) [1,2]. The availability and use of such materials could have a significant environmental impact, since it would drastically reduce wastes generated by conventional polymers [3]. Some of these biopolymers, such as PLA and native poly-saccharides, have the advantage of being biodegradable, which makes them interesting for various applications, especially packaging applications. Biopolymers are also used in many electronics applications as biodegradable substrates or insulating thin films to replace traditional polymers [4,5]. These applications often use films with thicknesses ranging from a few nanometers to a few micrometers. Since the operational temperature of devices can reach 100 °C (or even more) the determination of the thermal properties of these new polymers, especially their thermal conductivity, is very important to evaluate their ability to dissipate heating in electronic devices.

In this paper, two bio-based polymers, i.e. the polylactic acid (PLA) and the cellulose palmitate (CP), were studied by the 3-omega method to determine their thermal conductivity. The choice of these two biopolymers is motivated by the wish to replace conventional polymers (Kapton, PET, PEN, …) by bio-based polymers. The first one, PLA, is considered as a renowned biopolymer used in many fields including electronics. The second biopolymer of our choice, CP, is a new biopolymer whose thermal conductivity is unknown that could be of interest for future electronic or microfluidic applications. PLA is an easily biodegradable and hydrophilic biopolymer, unlike cellulose palmitate. The thermal conductivity of PLA has already been measured but mainly for PLA with nanocomposites or 3D printing PLA. In this last case, it is a heterogeneous material, composed of PLA and other additives in order to modify its properties like its adhesiveness, color or melting temperature. In the study proposed, PLA is prepared by casting method for making flexible transparent thick or thin films, and not blocs as it is the case in 3D printing.

Thermal conductivity can be determined by different methods. The first one is the time-domain thermoreflectance method. In this technique the sample is covered with a thin layer of metal and then is heated through a probe that generates ultra-short laser pulses [6]. The second one is the hot wire method. This method is based on the use of a transient radial flow technique to measure the thermal conductivity of

different materials and especially refractories, such as insulating bricks and powders or fibrous materials [7]. The third method is the guarded hot plate method. Its principle is to reproduce the uniform, unidirectional and constant thermal flux density existing through an infinite homogeneous slab-shaped specimen caught between two infinite isothermal planes [8]. Compared to other methods, the 3-omega method [9] is easy and accurate and it allows determining the thermal conductivity of both thin and bulk films which is of great interest when considering applications involving electronic devices. This method has already been successfully used to determine the thermal conductivity of classical polymers, such as polydimethylsiloxane [10], polymide [11] and polyaniline [12]. The 3-omega method can be also used to determine the thermal conductivity of fluids [13] and gas [14].

Thermal conductivities of bulk films can be substantially different from those of thin films, and these latter have gained growing importance in various applications. Therefore, it is necessary to measure the thermal conductivity of thin and thick biopolymer films. Thus both bulk and thin films of PLA and CP have been prepared and characterized. Thin films were deposited by spin-coating on the surface of borosilicate substrates [15]. The thermal conductivity was measured at room temperature.

2. Description of used biopolymers

2.1. Polylactic acid (PLA)

PLA is a bio-based thermoplastic polyester biologically obtained from renewable resources by fermentation of carbohydrate or starch by lactic bacteria. PLA is transparent and has good mechanical properties [16] as described in Table 1. It was first used in the medical field, especially according to its biocompatibility and biodegradability properties [17], but its sustainability and its decreasing production cost (related to the increase of its production volume) have opened a large range of potential application fields, such as food packaging, textile, automobile and electronic industries [16]. Therefore, there is a need to better understand and improve its properties to expand its industrial uses, including in micro- or nano-electronic fields. PLA used in this study was purchased from Goodfellow in granular form. The different films were prepared by casting, a method consisting in dissolution of the granules in a volatile solvent (chloroform) and then evaporation of this solvent at room temperature under atmospheric pressure.

2.2. Cellulose palmitate (CP)

Fatty acid cellulose esters (FACEs) are experimental products synthesized by grafting fatty acid chains, obtained by the hydrolyses of vegetal oil, onto cellulose, the most abundant natural polymer on Earth [18]. Cellulose palmitate, resulting from the coupling of cellulose with palmitic fatty chain, is a hydrophobic material. CP mechanical properties [18,19] are indicated in Table 1, and compared with PLA ones.

PLA and CP, both bio-based materials, are interesting to be used in such comparative study because their properties are mainly opposite:

- PLA is biodegradable, CP not.
- CP is very ductile and PLA is harder.

Table 1
Physical characteristics of PLA and CP.

Properties	PLA	CP
Elongation at break (%)	6.00	40.00
Young Modulus (GPa)	3.50	0.19
Tensile strength (MPa)	53.00	10.10
Density (g.cm^{-3})	1.24	0.94
Glass transition temperature (°C)	55.00	122.00
Contact angle θ (°)	80.00	103.00

- CP is clearly hydrophobic, PLA not (Contact angle θ < 90°).

The CP used is in the form of cotton. The different films are prepared by the same method used for the preparation of PLA films (casting in chloroform).

The 3-omega method requires the deposition of a metallic line on the films surface, usually performed by photolithography. In the case of biopolymers, this micro-fabrication process can damage the films because of chemical products and high temperatures. For this reason, an alternative micro-fabrication process was implemented. This process, explained in section 4, is based on the deposition of the metallic lines by evaporation through a shadow mask, placed close by the biopoylmer substrate.

3. Characterization method

3.1. 3-Omega method

Thermal conductivity is a physical property that describes the ability of a material to conduct heat. Today the 3-omega method is one of the most popular methods to measure thermal conductivity. It can be used to investigate thin films as well as thick films. This technique was first developed and reported by Cahill in 1987. In order to be implemented, a thin metallic line with at least 2 contact pads is deposited onto the surface of the substrate to be measured: a typical geometry is shown in Fig. 1. The metallic line acts both as heater and temperature sensor. When an alternating current $I_0 \cos(\omega t)$ is driven through it at an angular frequency ω (in rad/s), resistive heating generates oscillating resistance component at angular frequency 2ω. The resistance of the metallic line is then given by:

$$R(t) = R_0(1 + \beta_h \Delta T_{DC} + \beta_h \Delta T_{AC} \cos(2\omega t + \varphi)) \tag{1}$$

Where R_0 is the resistance of the metallic line at room temperature in Ω, β_h is the temperature coefficient of resistance of the metallic line in °C^{-1}, ΔT_{DC} is the DC temperature rise, ΔT_{AC} is the amplitude of the AC temperature oscillations, and ϕ is the phase shift between the oscillations heating power at angular frequency 2ω and the temperature oscillations of the metallic line. The voltage across the metallic line can be obtained by multiplying the heater resistance with the input current, resulting in:

$$V(t) = R(t) * I_0 \cos(\omega t) = R_0 I_0 \left[(1 + \beta_h \Delta T_{DC}) \cos(\omega t) \right.$$
$$\left. + \frac{1}{2}\beta_h \Delta T_{AC} \cos(\omega t + \varphi) + \frac{1}{2}\beta_h \Delta T_{AC} \cos(3\omega t + \varphi) \right] \tag{2}$$

Examining Eq. (2), we can express the 3ω amplitude as:

$$V_{3\omega} = \frac{1}{2} V_0 \beta_h \Delta T_{AC} \tag{3}$$

where $V_0 = R_0 I_0$ is the initial voltage applied to the metallic line. The in-phase and out-phase components of the temperature oscillations ΔT_{AC} can then be deduced by measuring the voltage at the 3ω frequency.

The magnitude of temperature oscillations at angular frequency 2ω over the metallic line can be determined by Refs. [9,20]:
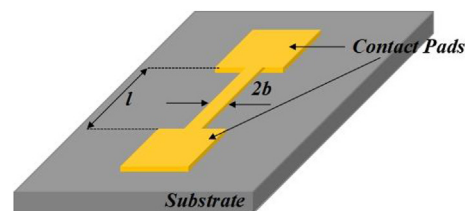

Fig. 1. Schematic of a metallic line deposited on a substrate used for 3-omega measurements, with length l and width $2b$.

$$\Delta T_{AC}(2\omega) = \frac{p_{rms}}{\pi k} \int\limits_{0}^{\infty} \frac{\sin^2(\eta b)}{(\eta b)^2 \sqrt{\eta^2 + q^2}} d\eta \qquad (4)$$

With $\quad q = \sqrt{\frac{i2\omega}{\alpha}} \quad$ and $\quad \alpha = \frac{k}{\rho c_p} \qquad (5)$

where k is the thermal conductivity of the substrate (in W/m.K), p_{rms} is the power supplied to the metallic line in W/m, and b is the half width of the metallic line. q is defined as the wavenumber of the thermal wave and α the thermal diffusivity in m^2/s.

When the thermal penetration depth λ is larger than the thin metallic line width, and lower than the thickness of the substrate (t_s) to prevent back surface reflections ($2b < \lambda < t_s$), Eq. (4) can be linearized. It can be expressed by Ref. [9]:

$$\Delta T_{AC}(2\omega) = \frac{-p_{rms}}{2\pi k}\left(\ln\left(\frac{b^2}{\alpha}\right) + \ln(2\omega) - 1.844\right) - i\frac{p_{rms}}{4k} \qquad (6)$$

We recall that the thermal penetration depth, λ (in meter), depends on the substrate thermal properties according to [19]:

$$\lambda = \sqrt{\alpha/2\omega} \qquad (7)$$

Eq. (6) proves that for the linear regime, the in-phase component decays logarithmically with respect to 2ω. However, over the same frequency range, the out-phase temperature oscillation is constant.

The boundary frequencies of the linear regime, for which the thermal conductivity can be measured, is calculated as:

$$\frac{25\alpha}{4\pi t_s^2} \le f \le \frac{\alpha}{100\pi b^2} \qquad (8)$$

Eq. (8), which gives boundary frequencies to estimate the linear frequency zone, requires the knowledge of the thermal diffusivity of the material under test. This value is taken from the literature if available. If not, a fast frequency sweep covering a wide band is made to locate the experimental linear zone. Then, a second sweep, finer, is made only in this area to acquire more measurement points and so to obtain a more accurate value of the thermal conductivity.

Substituting Eq. (6) into Eq. (3) yields the third harmonic voltage $V_{3\omega}$. After determining the slope of the experimental evolution of the in-phase harmonic 3ω voltage versus ln (2ω) within the linear zone, the thermal conductivity can be determined by Eq. (9) [21]:

$$k = \frac{V_0^3 \beta_h}{4\pi l R_0} * \frac{\ln\left(\frac{\omega_2}{\omega_1}\right)}{(V_{3\omega,1} - V_{3\omega,2})} \qquad (9)$$

where $V_{3\,\omega,1}$ and $V_{3\,\omega,2}$ are the in-phase third harmonic voltages measured at angular frequencies ω_1 and ω_2 respectively.

3.2. Application of the 3-omega method for thin films

Many methods have been performed to measure the thermal conductivity of thin films among which the 3 ω differential technique has been widely used [16]. Thermal conductivity of a thin film can be obtained by comparing the temperature oscillations of a film/substrate system with the corresponding value of the substrate alone. As shown in Fig. 2, a thin film of thickness t_f is deposited on the surface of a substrate of thickness t_s. When t_f is far smaller than the width of the metallic line 2 b ($t_f < < 2b$), a one dimensional heat flow will occur perpendicular to the film/metallic line interface. If the thermal conductivity of the thin film k_f is much smaller than that of the substrate material k_s, the temperature rise ΔT_f induced by the thin film is given by Ref. [22]:
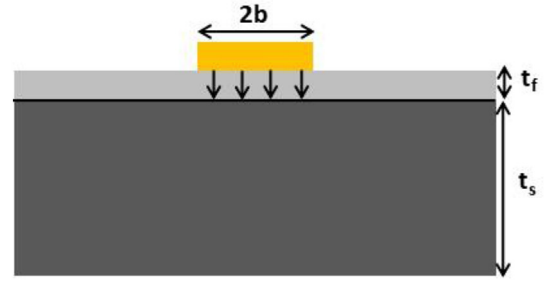
$$\Delta T_f = \frac{p_{rms}}{2b} \frac{t_f}{k_f} \qquad (10)$$

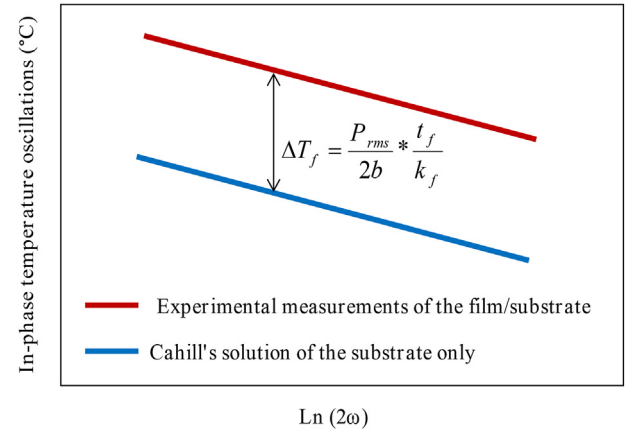**Fig. 2.** Thin film of thickness t_f deposited on a substrate of thickness t_s.

Fig. 3. Determination of the temperature rise ΔT_f.

The temperature ΔT_{AC} at the level of the metallic line is expressed as (see Fig. 3):

$$\Delta T_{AC} = \Delta T_f + \Delta T_s \qquad (11)$$

where ΔT_s is the temperature rise due to substrate alone.

To determine the thin film thermal conductivity k_f, the third harmonic voltage is initially measured for the film/substrate structure. Then, we determine the substrate thermal conductivity k_s by using Eq. (9). The in-phase temperature response ΔT_{AC} of the film/substrate structure is deduced from the measurement of the in-phase harmonic voltages $V_{3\omega}$ (Eq. (3)), while the temperature rise due to the substrate is calculated by using Cahill's formula (Eq. (6)), considering the value of the substrate thermal conductivity k_s previously calculated.

The difference between the two responses leads to the temperature rise due to the presence of the thin film; the thermal conductivity k_f can then be determined using the following equation [21]:

$$k_f = \frac{P_{rms}}{2b} * \frac{t_f}{\Delta T_f} \qquad (12)$$

4. Process description

4.1. Preparation of the biopolymer films

To measure the thermal conductivity of PLA and CP films, a solvent film casting technique was used to prepare bulk as well as thin films. PLA granules and CP powder are pre-treated in a desiccator for at least 12 h at room temperature, in order to keep the PLA granules and CP powder dry. Then they are dissolved in chloroform (PLA: 0,4 g/10 ml) (CP: 1 g/10 ml) in a glass flask. The two solutions are stirred using magnetic stir for three to 4 h until the biopolymers are completely dissolved. To obtain bulk films, the solutions are poured into two flat bottom glass beaker. At the end of the chloroform evaporation, bulk
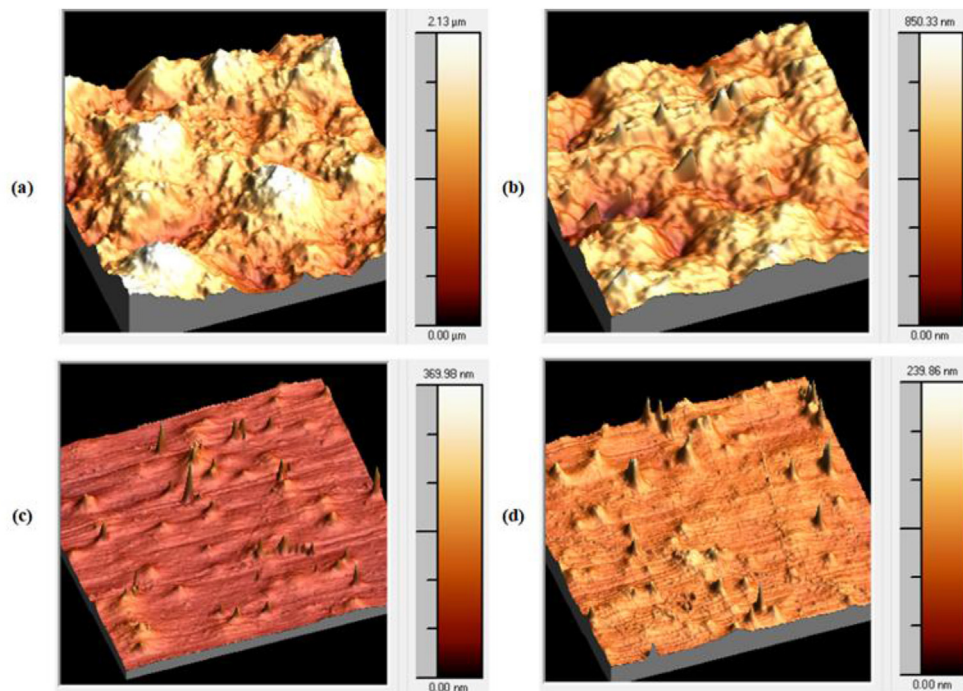
Fig. 4. Scanning probe microscopy images of (PLA, CP) thick films (a, b) before bonding, (c, d) after bonding respectively.

films are formed at the bottom of the glass beakers. All prepared films are stored at room temperature for 1 week to ensure the evaporation of residual chloroform.

Concerning PLA and CP thin films, they are deposited on borosilicate substrates. These latter are initially cleaned ultrasonically in acetone for 15 min and then in propanol-2 for 5 min. Then, the substrates are blown dry by compressed nitrogen. To insure the absence of any residues, a UV-ozone treatment is applied on the substrates for 15 min. Finally, the PLA and CP solutions are spin-coated onto the borosilicate substrates. Different spin-coating speeds were tested to obtain films with thicknesses around 200 and 250 nm. The PLA/Br and CP/Br samples are stored at room temperature for 48 h until the evaporation of chloroform.

After the preparation of the biopolymer samples, the metallic lines were deposited through a shadow mask by evaporation. To obtain uniform and continuous lines, the surface of the films must be flat. However, as can be seen on the images Fig. 4, the prepared thick films exhibit both a rough surface. This is related to the evaporation rate of the solvent and the surface state on which the polymers are poured. To lower the surface roughness of the biopolymer bulk films and to have flat films, a bonding technique is applied by using a wafer bonder machine (Suss MicroTec SB6e). The biopolymer film is bonded onto a silicone substrate by applying high temperature and pressure. This technique allows approaching the roughness of the material used for the bonding. The choice of silicone permits thus to have a flat film that presents a good surface state.

Different pressures and temperatures were used to keep thick substrates. PLA and CP were respectively laminated at 100 °C and 120 °C under 2-bar pressure for 15 min. Then, the film is peeled off from the silicon substrate. At the end of the process, the thicknesses of PLA and CP films are 550 µm and 700 µm respectively. A scanning force microscope image has been made for the both bulk films, before and after the bonding. Fig. 4 shows the surface morphologies of PLA (Fig. 4a) and CP (Fig. 4b), before the bonding. It can be clearly seen that both samples contained many packed microspheres and deep pits. In Fig. 4c and d, after the bonding, the surfaces of the samples appeared more flat and some irregular peaks were also present. These latter are related to the measurements, but they have no significant impact on the roughness

Table 2
Roughness values before and after bonding (RMS).

Bulk Biopolymer films	Roughness values (nm)	
	Before bonding	After bonding
PLA	320	14
CP	105	12

values (RMS) (Table 2). Comparatively, the surface of both thin films is flat, due to the very small film thickness and to the high evaporation rate of the solvent. So, no treatment was applied to the films after the deposition on the borosilicate substrate.

This technique allows a reduction of the roughness values of the thick films of 95% for PLA and of 88% for CP.

4.2. Metallic lines deposition through shadow mask

The metallic lines were deposited through a 30 µm thick nickel shadow mask, illustrated in Fig. 5a, purchased by Temicon GmbH.
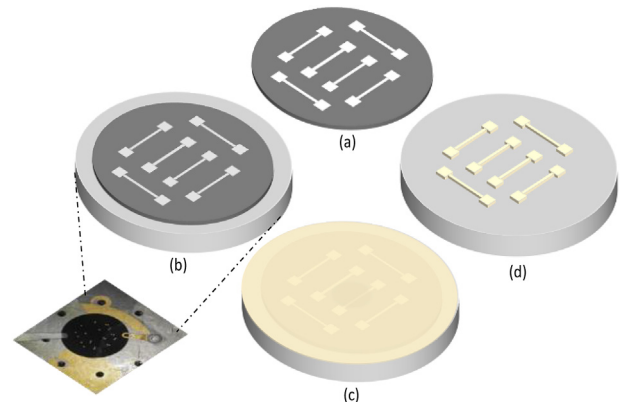

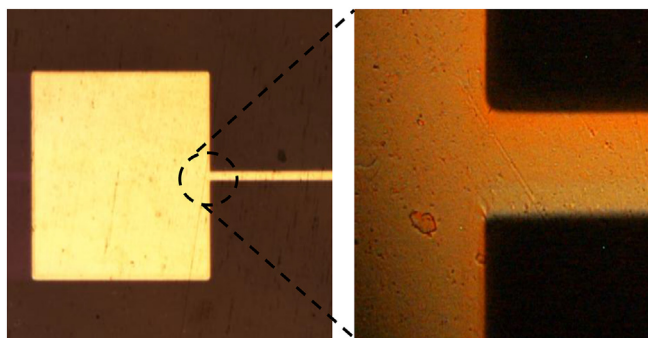Fig. 5. Steps of metallic lines patterning using nickel shadow mask.

Fig. 6. Optical images of a metallic line patterned on PLA bulk film.

Fig. 8. SEM image of a metallic line patterned on CP bulk film.

Fig. 5 illustrates the steps for line patterning utilizing this shadow mask. First, the mask is placed in contact with the biopolymer where the patterning is needed as shown in Fig. 5b and fixed mechanically to the substrate. Then, two metal layers of 50 nm titanium (Ti) as adhesion layer and 450 nm gold (Au) layer, were deposited subsequently by electron beam evaporation over the shadow mask as seen in Fig. 5c. Finally, the mask is carefully peeled off from the substrate leaving patterned gold lines on it as shown in Fig. 5d. The shadow mask was cleaned ultrasonically in acetone for 15 min and then in propanol-2 for 5 min, to ensure the elimination of all residues within the openings and was after that step ready for reuse.

Fig. 6 shows optical microscope images of metallic lines deposited on PLA substrate. The widths of the obtained gold lines exceed those of the designed openings through the shadow mask, except for some lines deposited on cellulose palmitate thin film.

This is attributed, on the one hand to the position of the evaporation source, on the other hand to the presence of a gap between the mask and the substrate which cannot be put together in perfect contact.

Furthermore, as seen in Fig. 7b a metallic line deposited on CP thin film was somewhat damaged at the removing of the shadow mask from the biopolymer substrate, but this effect can be neglected for the widest lines. However, the method used remains reliable, as 80% of the metallic lines are not damaged. In the study only these latter are used for the tests. So, as just the uniform lines along the length are investigated, there is no contribution of this parameter (width along the length) to the measurement error.

In addition to the optical image, Fig. 8 shows a SEM image of a metallic line on CP bulk film. As mentioned above, the widths of the metallic lines do not correspond exactly to those of the shadow mask what causes a shadowing effect. The metallic lines are narrow on the top compared to the bottom, specially, for the largest metallic lines for which we can notice that this effect is more pronounced. For thick films, since the width 2 b is not included in Eq. (9), it does not impact
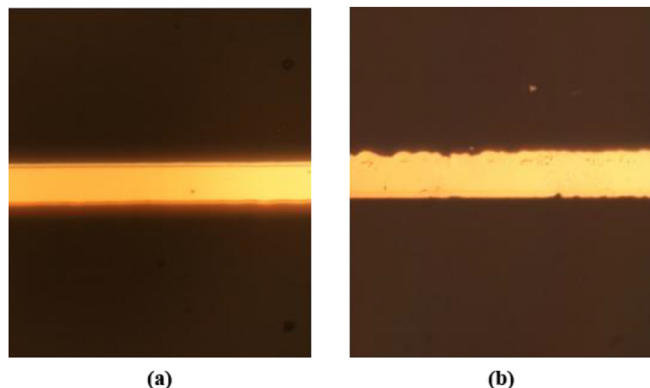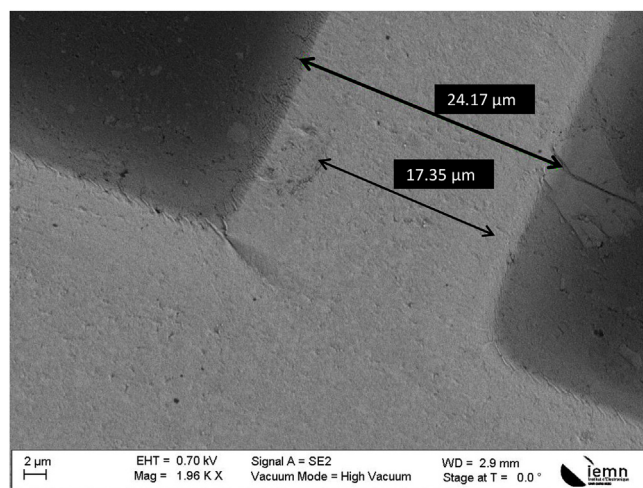
Table 3
Dimensions of metallic lines deposited on bulk films.

	Polylactic Acid		Cellulose Palmitate	
Line	L1	L2	L3	L4
l (mm)	5	2.5	5.5	2.5
2 b (µm)	16	21	18	24

Table 4
Dimensions of metallic lines deposited on thin films.

	Polylactic Acid		Cellulose Palmitate	
Line	L5	L6	L7	L8
l (mm)	5	5	5.5	5
2b (µm)	26	30	17	9

the thermal conductivity value. For thin films, the knowledge of the width 2 b is needed, so the values given in the Table 3 (maximal width) are used to measure the thermal conductivity.

We performed measurements on several lines of different dimensions. Tables 3 and 4 present examples of dimensions for two lines of each sample. In these tables, 2 b is the maximal width of the metallic line.

5. Measurement results

Fig. 9 shows a schematic of the measurement setup used to extract the 3ω component of the voltage along the metallic line. Two AD 624 differential amplifiers are used to isolate the voltages across a variable resistor R_v and the metallic line. The outputs of the differential amplifiers are connected to the inputs A and B of the lock-in amplifier and differentiated through (A-B) mode. A function generator drives an alternating current through the metallic line causing temperature oscillations into the line. The variable resistor R_v is adjusted until reading a minimum voltage at a frequency ω, at the output of the lock-in amplifier. At this moment the variable resistance R_v is equal to the resistance of the metallic line. Then, the third harmonic voltage $V_{3\omega}$ only generated by the metallic line can be measured. In this study the frequency does not exceed 200 Hz.

In order to calculate the thermal conductivity of biopolymer films, we start by measuring the metallic line resistance R_0 by the 4-wire method at room temperature, using a micro-ohmmeter. Then, the metallic line is connected to the differential amplifier circuit. The initial voltage applied to the metallic line V_0 is determined in the (V_A) mode of the lock-in amplifier.

Fig. 7. Example of an optical image of metallic lines patterned on PLA thin film (a), and CP thin film (b).

Fig. 9. Schematic of the measurement setup.
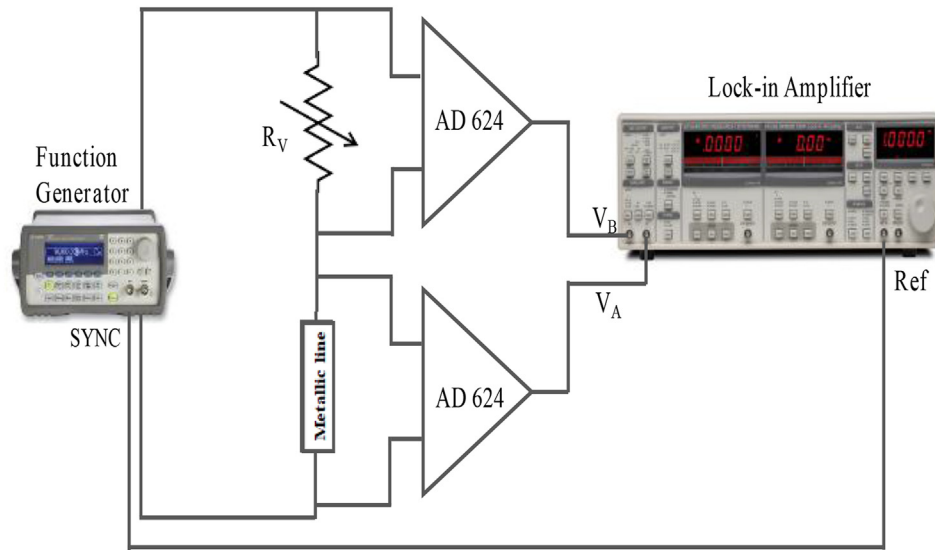
The in-phase and out-of-phase third harmonic voltage are then recorded within the linear regime. The limit frequencies are calculated by using Eq. (8), where the thermal diffusivity, taken from the literature, is close to $8.064.10^{-8}$ m²/s for PLA [23–25]. But for CP, the thermal diffusivity is not known. To obtain an estimation of the linear frequency zone, we took into account the properties of other cellulose esters which look like CP (cellulose acetate) [26,27]. The thermal diffusivity of cellulose acetate is between $8.38 \ 10^{-8}$ m²/s and $1.8 \ 10^{-7}$ m²/s [27]. Furthermore, the limit frequencies of the thin film on borosilicate substrate were determined by using the thermal diffusivity of borosilicate $6.875.10^{-7}$ m²/s [28].

At the end of the $V_{3\omega}$ measurement, the temperature coefficient of resistance β_h is determined by using the hot plate method with 4 wires connected to a micro-ohmmeter. The temperature measurements are accomplished by several thermocouples connected with thermal past just near the metal line. The resistance of the metallic line is measured with increasing temperature. The temperature coefficient of resistance can be calculated by Ref. [29]:

$$\beta_h = \frac{1}{R_0} \frac{dR}{dT} \tag{13}$$

Table 5 presents the values of the measured resistance R_0 at room temperature, the voltage V_0 applied on each metallic line, the temperature coefficient of resistance β_h and the rms power per meter applied on each metallic line on the bulk films (PLA, CP) and the thin film-on-substrate (PLA/Br, CP/Br).

The biopolymers PLA and CP have a low thermal conductivity. Therefore, the metallic line resistances were fed by a low power in

order to avoid excessive heating of the metallic line itself.

Fig. 10 presents the measurement results of the in-phase harmonic voltages versus Ln (2ω) for PLA (L1) and CP (L3) bulk films in the linear zone. The linear zone of bulk films ranges from 0.53 Hz to 4 Hz for PLA (L1) and from 0.54 Hz to 6.05 Hz for CP (L3). The fact that the
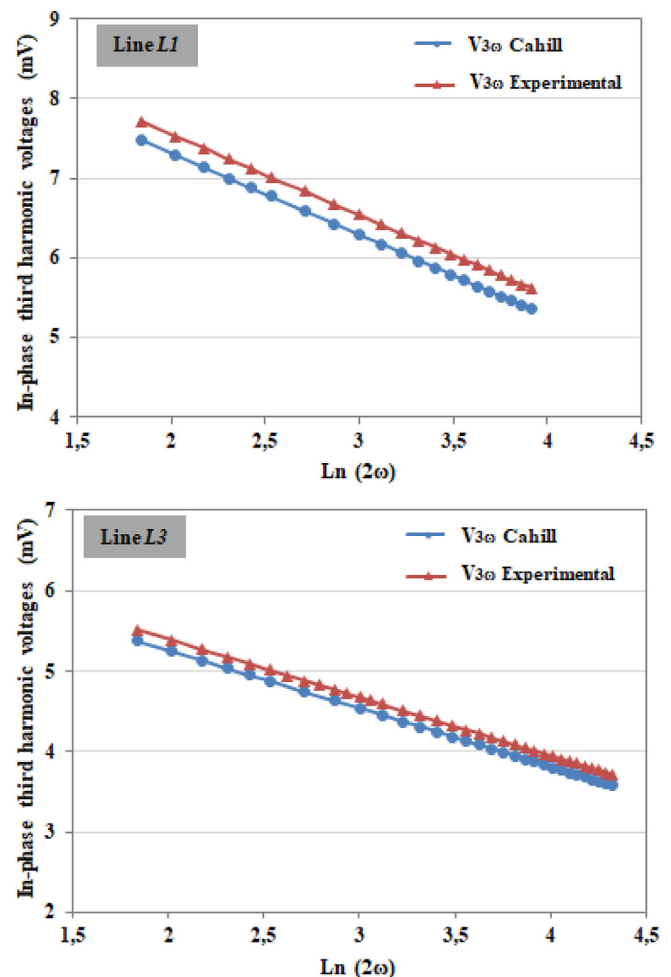

Fig. 10. The in-phase third harmonic voltages measured for PLA and CP bulk films, compared to Cahill's solution in linear zone.

Table 5
Properties of metallic lines.β

Samples	Line	R_0 (Ω)	β_h (°C⁻¹)	V_0 (V)	p_{rms} (W/m)
PLA	L1	14.975	0.00302	0.389	2.03
	L2	10.699	0.00295	0.296	3.28
CP	L3	44.521	0.00296	0.609	1.52
	L4	17.952	0.00289	0.445	4.42
PLA/Br	L5	23.123	0.00303	0.463	1.86
	L6	18.089	0.00307	0.408	1.85
CP/Br	L7	38.130	0.00271	0.554	1.47
	L8	78.784	0.00267	0.707	1.27

Table 6
Thermal conductivity of bulk films.

	Polylactic Acid		Cellulose Palmitate	
Line	L1	L2	L3	L4
Thermal conductivity (W/m.K)	0.188	0.195	0.300	0.304

measurements were performed at low frequency allows for very stable measurements. The thermal conductivity of the samples can be determined directly by using Eq. (9). The average value of the measured thermal conductivity is around 0.19 W/m.K for PLA and 0.30 W/m.K for CP. Table 6 presents the values of thermal conductivity measured for each of metallic lines on bulk films.

In order to validate the results, a comparison between the measured values of the in-phase third harmonic voltage $V_{3\omega}$ and the Cahill solution using Eq. (6) and Eq. (3) has been done. A MATLAB program has been written for comparison. Several measurement points have been cared. The measurements show a good agreement with the data obtained from Cahill's solution using the experimental values of the thermal conductivity and Eq. (6). The shift observed between the two lines is quite small. This demonstrates that the method proposed using shadow mask allowed us to have good results.

As we said before, the thermal conductivities of the bulk and thin films are different. Therefore, after determining the thermal conductivity of bulk biopolymers films, we measure the thermal conductivity of thin films by using the differential 3ω method proposed by Cahill as presented in section 2.4.

Firstly, we determine the thermal conductivities of substrate k_s of PLA/Br and CP/Br devices by using Eq. (9). The thermal conductivity measured for borosilicate was around 1.16 W/m.K, which is similar to the value found in the literature [28]. Then, the temperature oscillation in a film/substrate structure ΔT_{AC} was deduced from the measurement of the in-phase third harmonic voltages by using Eq. (14).

$$\Delta T_{AC} = \frac{2V_{3\omega}}{V_0 \beta_h} \tag{14}$$

This temperature oscillation ΔT_{AC} was compared with the corresponding value of the substrate oscillation temperature ΔT_S calculated according to Cahill using the measured thermal conductivity of the substrate and Eq. (6) (in MATLAB).

Fig. 11 presents the temperature oscillations of lines L5 and L7. The straight line with red triangles represents the experimental temperature oscillations ΔT_{AC} in the metallic line, deduced from the measured third harmonic voltages $V_{3\omega}$, whereas the straight line with blue circles represents the temperature oscillations ΔT_S over borosilicate substrate, calculated according to Cahill's solution.

The temperature rise ΔT_f determined by $\Delta T_f = \Delta T_{AC} - \Delta T_S$ is found to be 0.130 °C for PLA/Br and 0.097 °C for CP/Br. The thickness t_f of PLA and CP is 200 nm and 250 nm respectively. The thermal conductivity of thin films is determined using Eq. (12). Table 7 shows that the average values are 0.12 W/m.K for PLA thin film and 0.22 W/m.K for CP thin film which is 30% lower than the values for bulk films. This diminution is probably due to the difference of thermal transport, ensured by lattice vibrations (namely phonons), in thin and thick polymers films. So, in a first assumption, the decrease of the thermal conductivity of thin films compared to the one of bulk films can be attributed to the reduction of the phonon mean free path, which can be correlated to the microstructure of the films [30].

The results obtained of the thermal conductivities are compared to the values found in literature. For PLA (0.13–0.16 W/m.K) [22,23], a slight difference can be noticed. Actually, PLA characterizations are often performed on 3D printing PLA or PLA including nanoparticles. As, in both cases, some additives (or materials) are added in order to modify their properties [31–33], the results can be slightly different. Concerning the thermal conductivity of CP, we compared our values
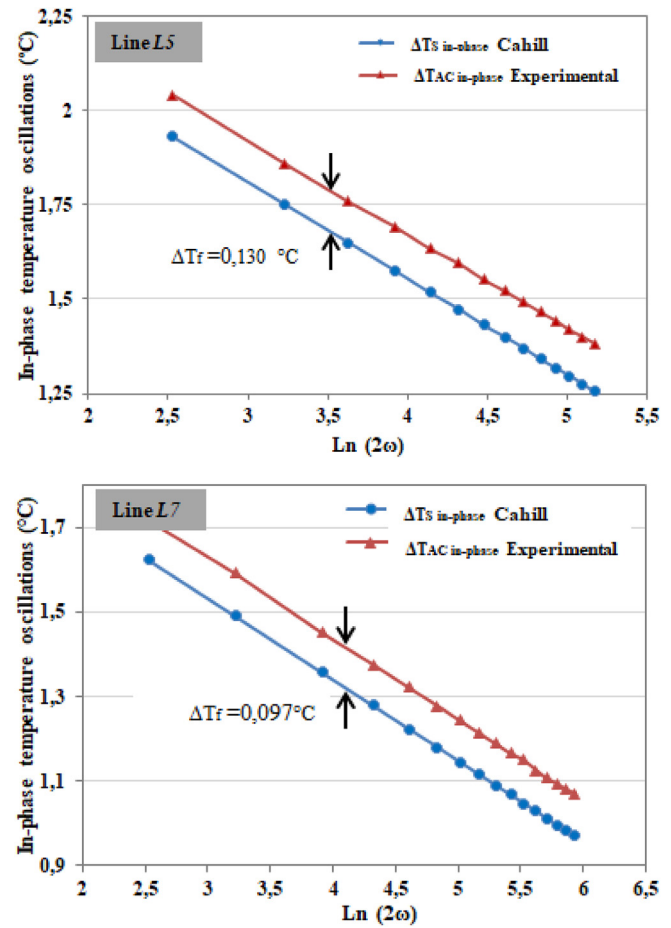

Fig. 11. Temperature oscillations of lines L5 and L7 patterned on thin films.

Table 7
Thermal conductivity of thin films.

	Polylactic Acid		Cellulose Palmitate	
Line	L5	L6	L7	L8
Thermal conductivity (W/m.K)	0.121	0.119	0.221	0.212

with those of cellulose acetate (0.16–0.33 W/m.K) [25,26]. These last ones present a good agreement. Another important point of this study is that, in this investigation, the biopolymer flexible films are prepared by casting method, while in Refs. [22,23,25,26] the films are prepared by compression molding which can also explain the small discrepancy in the results.

All these results show the importance of characterizing thick and thin films materials and the reliability of our fabrication process.

6. Conclusion

The thermal conductivity of polylactic acid and cellulose palmitate thick and thin films was measured at room temperature. For that purpose, the 3-omega method was used for bulk films whereas a differential 3-omega method was applied for thin films. The characterized films were prepared by dissolving biopolymers in chloroform. In addition, a bonding technique was used to improve the surface roughness of the biopolymer bulk films. Thin films were spin-coated on borosilicate substrates.

Stencil lithography based on the use of a Nickel shadow mask was applied to obtain metallic lines, which is suitable and compatible for fabricating micro-structures on the top of biopolymer films. The

experimental results of the third harmonic voltage were used to extract PLA and CP films thermal conductivity. This latter shows a good agreement with Cahill's solution. The average values of thermal conductivity are 0.19 W/m.K and 0.12 W/m for PLA bulk and thin films respectively, and 0.30 W/m.K and 0.22 W/m for CP bulk and thin films respectively.

This study exhibits thermal conductivities comparable to those of PEN and polyimide which are largely used in flexible electronics. So, these two biopolymers are promising alternatives to the petro-sourced polymers.

Acknowledgements

References

[1] M. Niaounakis, Biopolymers: Applications and Trends, William Andrew, 2015.

[2] E.E. Tanase, M. Rapa, O. Popa, Biopolymers based on renewable resources-A review, Sci. Bull. Biotechnol. 18 (2014) 188–195.

[3] A.K. Mohanty, M. Misra, L.T. Drzal, Sustainable bio-composites from renewable resources: opportunities and challenges in the green materials world, J. Polym. Environ. 10 (2002) 19–26.

[4] C.M. Boutry, A. Nguyen, Q.O. Lawal, A. Chortos, Z. Bao, Fully biodegradable pressure sensor, viscoelastic behavior of PGS dielectric elastomer upon degradation, SENSORS, 2015 IEEE, IEEE, 2015, pp. 1–4.

[5] G. Mattana, D. Briand, A. Marette, A. Vásquez Quintero, N.F. de Rooij, Polylactic acid as a biodegradable material for all-solution-processed organic electronic devices, Org. Electron. 17 (2015) 77–86.

[6] P.E. Hopkins, B. Kaehr, L.M. Phinney, T.P. Koehler, A.M. Grillet, D. Dunphy, F. Garcia, C.J. Brinker, Measuring the thermal conductivity of porous, transparent SiO2 films with time domain thermoreflectance, J. Heat Tran. 133 (2011) 061601-061601-8.

[7] A. Franco, An apparatus for the routine measurement of thermal conductivity of materials for building application based on a transient hot-wire method, Appl. Therm. Eng. 27 (2007) 2495–2504.

[8] D. Salmon, Thermal conductivity of insulations using guarded hot plates, including recent developments and sources of reference materials, Meas. Sci. Technol. 12 (2001) R89.

[9] D.G. Cahill, Thermal conductivity measurement from 30 to 750 K: the 3ω method, Rev. Sci. Instrum. 61 (1990) 802–808.

[10] N. Al-Khudary, P.Y. Cresson, Y. Orlic, P. Coquet, P. Pernod, T. Lasri, Measurement of the thermal conductivity of polydimethylsiloxane polymer using the three omega method, Key Eng. Mater. 613 (2014) 259–266.

[11] N. Al-Khudary, P.Y. Cresson, W. Wei, H.G. Happy, T. Lasri, Inkjet printing technology for polymer thermal conductivity measurement by the three omega method, Polym. Test. 40 (2014) 187–195.

[12] P.B. Kaul, K.A. Day, A.R. Abramson, Application of the three omega method for the thermal conductivity measurement of polyaniline, J. Appl. Phys. 101 (2007) 083507.

[13] S.-M. Lee, Thermal conductivity measurement of fluids using the 3ω method, Rev.

Sci. Instrum. 80 (2) (2009) 024901.

[14] E. Yusibani, P.L. Woodfield, M. Fujii, K. Shinzato, X. Zhang, et Y. Takata, Application of the three-omega method to measurement of thermal conductivity and thermal diffusivity of hydrogen gas, Int. J. Thermophys. 30 (2) (2009) 397–415.

[15] D.G. Cahill, M. Katiyar, J.R. Abelson, Thermal conductivity of a-Si: H thin films, Phys. Rev. B 50 (1994) 6077.

[16] R.A. Auras, L.-T. Lim, S.E.M. Selke, H. Tsuji, Poly (Lactic Acid): Synthesis, Structures, Properties, Processing, and Applications, John Wiley & Sons, 2011.

[17] Y. Ramot, M. Haim-Zada, A.J. Domb, A. Nyska, Biocompatibility and safety of PLA and its copolymers, Adv. Drug Deliv. Rev. 107 (2016) 153–162.

[18] L. Crépy, V. Miri, N. Joly, P. Martin, J.-M. Lefebvre, Effect of side chain length on structure and thermomechanical properties of fully substituted cellulose fatty esters, Carbohydr. Polym. 83 (2011) 1812–1820.

[19] L. Crépy, L. Chaveriat, J. Banoub, P. Martin, N. Joly, Synthesis of cellulose fatty esters as plastics—influence of the degree of substitution and the fatty chain length on mechanical properties, ChemSusChem 2 (2009) 165–170.

[20] K. Valalaki, A.G. Nassiopoulou, Improved approach for determining thin layer thermal conductivity using the 3 ω method. Application to porous Si thermal conductivity in the temperature range 77–300 K, J. Phys. D Appl. Phys. 50 (2017) 195302.

[21] D.G. Cahill, R.O. Pohl, Thermal conductivity of amorphous solids above the plateau, Phys. Rev. B 35 (1987) 4067–4073.

[22] Z.-X. Zong, Z.-J. Qiu, S.-L. Zhang, R. Streiter, R. Liu, A generalized 3ω method for extraction of thermal conductivity in thin films, J. Appl. Phys. 109 (2011) 063502.

[23] B. Mortazavi, F. Hassouna, A. Laachachi, A. Rajabpour, S. Ahzi, D. Chapron, V. Toniazzo, D. Ruch, Experimental and multiscale modeling of thermal conductivity and elastic properties of PLA/expanded graphite polymer nanocomposites, Thermochim. Acta 552 (2013) 106–113.

[24] S.G. Mosanenzadeh, S. Khalid, Y. Cui, H.E. Naguib, High thermally conductive PLA based composites with tailored hybrid network of hexagonal boron nitride and graphene nanoplatelets, Polym. Compos. 37 (2016) 2196–2205.

[25] Polylactic Acid (PLA, Polylactide): MakeItFrom.com». https://www.makeitfrom.com/material-properties/Polylactic-Acid-PLA-Polylactide.

[26] J. Clemens, M. Lasance, The thermal conductivity of unfilled plastics, Technical Data 7 (2001).

[27] Propeties: Cellulose acetate. https://www.azom.com/properties.aspx?ArticleID=1461.

[28] D. Hartung, F. Gather, P.J. Klar, Comparison of different methods for measuring thermal conductivities, 9th European Conference on Thermoelectric AIP Conf.Proc vol 1449, (2012), pp. 381–384.

[29] A. Jacquot, B. Lenoir, A. Dauscher, M. Stölzer, J. Meusel, Numerical simulation of the 3ω method for measuring the thermal conductivity, J. Appl. Phys. 91 (2012) 4733–4738.

[30] L. Bai, X. Zhao, R.-Y. Bao, Z.-Y. Liu, M.-B. Yang, W. Yang, Effect of temperature, crystallinity and molecular chain orientation on the thermal conductivity of polymers: a case study of PLLA, J. Mater. Sci. 53 (14) (2018) 10543–10553.

[31] Flaata T., Michna G. J., Letcher T., Thermal conductivity testing apparatus for 3D printed materials, ASME 2017 Summer Heat Transfer Conference July 9-14, 2017, Bellevue, Washington, USA.

[32] S.M. Lebedev, O.S. Gefle, E.T. Amitov, D.Yu Berchuk, D.V. Zhuravlev, Poly(lactic acid)-based polymer composites with high electric and thermal conductivity and their characterization, Polym. Test. 58 (2017) 241–249.

[33] Y. Gao, O.T. Picot, E. Bilotti, T. Peijs, Influence of filler size on the properties of poly (lactic acid) (PLA)/graphene nanoplatelet (GNP) nanocomposites, Eur. Polym. J. 86 (2017) 117–131.